Regular Article

PC3-Secreted Microprotein Is Expressed in Glioblastoma Stem-Like Cells and Human Glioma Tissues

Masato Maruyama,*[,a,†] Yousuke Nakano,[a] Takuya Nishimura,[a] Ryoichi Iwata,[b] Satoshi Matsuda,[c] Mikio Hayashi,[d] Yuki Nakai,[a] Masahiro Nonaka,[b] and Tetsuo Sugimoto[a,‡]

[a] *Department of Anatomy and Brain Science, Kansai Medical University; 2–5–1 Shinmachi, Hirakata, Osaka 573–1010, Japan:* [b] *Department of Neurosurgery, Kansai Medical University; 2–5–1 Shinmachi, Hirakata, Osaka 573–1010, Japan:* [c] *Department of Cell Signaling, Institute of Biomedical Science, Kansai Medical University; 2–5–1 Shinmachi, Hirakata, Osaka 573–1010, Japan: and* [d] *Department of Physiology, Kansai Medical University; 2–5–1 Shinmachi, Hirakata, Osaka 573–1010, Japan.*

Received October 28, 2020; accepted April 15, 2021; advance publication released online April 23, 2021

Glioblastoma multiforme (GBM) is the most prevalent malignant primary brain tumor with a high recurrence rate. Despite multimodal therapy including surgical resection, chemotherapy, and radiotherapy, the median survival time after the initial diagnosis of GBM is approximately 14 months. Since cancer stem cells (CSCs) are considered the leading cause of cancer recurrence, glioblastoma stem cell-targeted therapy is a promising strategy for the treatment of GBM. However, because CSC heterogeneity has been implicated in the difficulties of CSC-target therapy, more in-depth knowledge of CSC biology is still required to develop novel therapies. In this study, we established single cell-derived tumorspheres from human glioblastoma U87MG cells. One of these tumorspheres, P4E8 clone, showed CSC-like phenotypes, such as self-renewal capacity, expression of CSC markers, resistance to anti-cancer agents, and *in vivo* tumorigenicity. Therefore, we used P4E8 cells as a cell-based model of glioblastoma stem cells (GSCs). Gene expression analysis using microarray indicated that the most highly expressed genes in P4E8 cells compared to the parental U87MG were PC3-secreted microprotein (MSMP). Furthermore, MSMP was expressed in patient-derived GSCs and human glioma tissues at the protein level, implying that MSMP might contribute to glioma development and progression.

Key words glioblastoma; cancer stem-like cell; PC3-secreted microprotein; tumorsphere; DNA microarray

INTRODUCTION

Glioblastoma multiforme (GBM) is the most common and aggressive primary brain tumor. The median overall survival of patients who received multimodal therapy including surgery, radiotherapy and chemotherapy, is approximately 14.6 months.[1)] Accumulating evidence indicated that cancer stem cells (CSCs), a small subpopulation of tumor cells, are present in many types of solid tumors including GBM. CSCs can generate a tumor through self-renewal ability, multi-lineage differentiation potential, and play a critical role in tumor development. In addition, since CSCs are resistant to conventional chemotherapy and radiation treatments, the remaining CSCs after surgery can cause a tumor recurrence.[2)] Therefore, targeted therapies against CSCs are considered to be a promising therapeutic strategy.[3)]

To isolate CSCs, various approaches, including cell sorting with antibodies against specific cell surface markers by fluorescence activating cell sorting (FACS) and side population (SP) assay, have been employed. However, these methods are sometimes limited by phenotypic heterogeneity of CSCs. For instance, although CD133 was widely used as a CSC marker in glioblastoma, the CD133-negative cell population also exhibited stem cell characteristics and tumorigenicity.[4,5)] The SP assay is based on the high efflux ability of fluorescent dye in stem cells and several reports had indicated that stem-like cell population was isolated from cancer cell lines and tumor tissues by SP assay,[6–8)] but other report had shown that SP cells did not contribute to CSC phenotype.[9)]

On the other hand, sphere formation assay was also used to isolate CSCs. This method was based on the resistance of stem cells to anoikis, a kind of apoptosis. When cell attachment or cell–matrix interaction was disrupted, anchorage-dependent differentiated cells induce anoikis, whereas stem cells survive and proliferate.[10)] However, anchorage-dependent cells can adhere together to survive and proliferate in floating cell culture conditions.[11,12)] Therefore, one promising approach to isolate CSCs is considered to form single-cell-derived tumorsphere because aggregation of anchorage-dependent cells must be prevented.[13,14)] In fact, this approach succeeded in the establishment of CSC lines from human colon cancer cell line,[15)] human primary colorectal cancer,[16)] human liver cancer,[17)] and human glioblastoma.[18)]

In this study, we established single cell-derived tumorspheres from human glioblastoma cell line U87MG, and one of the established tumorsphere, P4E8, showed CSC-like properties. To find novel therapeutic target molecules, we performed differential gene expression analysis between U87MG and P4E8 cells and identified that the most highly expressed

† Present address: *Department of Pharmaceutics, Faculty of Pharmaceutical Sciences, Okayama University; 1–1–1 Tsushima-naka, Kita-ku, Okayama 700–8530, Japan.*

‡ Present address: *Departments of Anatomy and Brain Science, and Fundamental Nursing, Kansai Medical University; Hirakata, Osaka 573–1004, Japan.*

* To whom correspondence should be addressed. e-mail: maruyamm@okayama-u.ac.jp

gene in P4E8 cells was PC3-secreted microprotein (MSMP). Immunostaining analysis further indicated that the expression of MSMP in patient-derived glioma stem cells (GSCs) and human glioma tissues.

MATERIALS AND METHODS

Cell Culture Human glioblastoma U87MG cells were obtained from European Collection of Cell Cultures (ECACC, Wiltshire, U.K.) and were maintained in Minimum Essential Medium (MEM; Sigma, St. Louis, MO, U.S.A.) supplemented with 10% fetal bovine serum (FBS), 1% non-essential amino acid (Gibco, Thermo Fisher Scientific, Waltham, MA, U.S.A.), 1 mM sodium pyruvate (Nacalai Tesque, Kyoto, Japan), and 100 U/mL penicillin, 100 μg/mL streptomycin (Invitrogen, Thermo Fisher Scientific) in humidified air atmosphere containing 5% CO_2 at 37 °C. Single cell-derived U87MG clones and previously established patient-derived GSC lines (146, MD13) (kind gifts from Dr. Ichiro Nakano, University of Alabama at Birmingham)[19] were cultured as floating sphere in neurosphere medium (Dulbecco's modified Eagle's medium/F12 supplemented with 1% N2 Max Media Supplement (R&D Systems, Minneapolis, MN, U.S.A.), 2% B27 Supplement Minus Vitamin A (Thermo Fisher Scientific), 3 mM sodium bicarbonate, 100 U/mL penicillin, 100 μg/mL streptomycin, 20 ng/mL basic fibroblast growth factor and epidermal growth factor (EGF). Human embryonic stem cell (H9)-derived neural stem cells (hNSC) (Thermo Fisher Scientific) were cultured according to the manufacturer's protocol.

Establishment of Single Cell-Derived Tumorspheres from U87MG Cells U87MG cells dissociated with Accutase (Innovative Cell Technologies, San Diego, CA, U.S.A.) were washed twice with ice-cold 2% FBS-phosphate-buffered saline (PBS) and stained with 7-aminoactinomycin D (7-AAD) (BD Biosciences, Franklin Lakes, NJ, U.S.A.) to exclude dead cells. Cells were first gated by forward *versus* side scatter (FSC-A *vs.* SSC-A) to exclude cellular debris. Single cells were then separated from doublets by two subsequent gates in plot of FSC-A *vs.* FSC-W and SSC-A *vs.* SSC-W. Finally, 7-AAD-negative live cells were sorted into 150 μL of neurosphere medium in 96-well suspension culture plates (Sumilon, Sumitomo Bakelite, Tokyo, Japan) using a FACS Aria IIμ (Becton Dickinson, San Jose, CA, U.S.A.). After two weeks, the phase contrast image of each sphere was observed, and the diameters were measured using a Leica AF7000 fluorescent microscope (Leica, Heerbrugg, Switzerland). Individual spheres were expanded and used for further experiments.

Xenotransplantation All animal experiments were approved by the Animal Care and Use Committee of Kansai Medical University (No. 14-121) and performed in accordance with the institutional guidelines. Six- to eight-week-old female BALB/c nude mice (BALB/c slc-nu/nu, Shimizu Laboratory Supplies Co., Ltd., Kyoto, Japan) were used in this study. After U87MG cells and tumorspheres were dissociated with Accutase, cells (3×10^5 or 1×10^6) in 100 μL of PBS were subcutaneously injected into the left flanks of the mice. The same amount of PBS was injected into the right flank as a control. Tumor volume was measured every 5 d and calculated using the following formula: $V\ (\mathrm{mm}^3) = 1/2(D \times d^2)$ where D and d are the longest and the shortest diameters, respectively. To assess tumor-initiating ability, mice bearing tumors larger than 100 mm^3 were counted as tumor-bearing mice.

For the orthotopic implantation, cells (5×10^5 cells in 2 μL of PBS) were stereotactically injected into the right striatum of mice under anesthesia with the mixture of midazolam, medetomidine, and butorphanol. After 14 d, the mice were deeply anesthetized and sacrificed with carbon dioxide. The mice were then perfused transcardially with PBS, followed by 4% paraformaldehyde. The brain was dissected out and immersed in 4% paraformaldehyde overnight at 4 °C. After embedded in paraffin, coronal sections (5 μm in thickness) were prepared and stained with hematoxylin–eosin (H&E) staining to indicate the tumor area.

Immunocytochemistry Cells seeded onto 8-well chamber slides (Matsunami Glass Industry, Osaka, Japan) (double-coated with 15 μg/mL poly-L-ornithine and 10 μg/mL laminin) were fixed with 4% paraformaldehyde and permeabilized with 0.2% Triton X-100. After blocking with Blockace (Dainippon Pharmaceutical, Osaka, Japan), cells were incubated with primary antibodies at 4 °C overnight, followed by the appropriate secondary antibodies. Antibodies used are listed in Supplementary Table 1. Cell nuclei were stained by incubation with 2 μM Hoechst33342 for 30 min at room temperature, following treatment with secondary antibody. Fluorescence images were acquired by the LSM 700 confocal microscope (Carl Zeiss Microscopy GmbH, Jena, Germany).

Limiting Dilution Assay Limiting dilution assay was performed as previously described.[20] Briefly, cells were dissociated with Accutase and plated on 96 well plates in two-fold serial dilution ranging from 0.98–500 cells/well in neurosphere medium. After 6 d, the number of wells without spheres were counted and plotted against the number of cells per well. The number of cells required to form at least one tumorsphere was calculated from the point at which 37% of the well did not have tumorspheres.

Cell Viability Assay Cells were seeded onto poly-L-ornithine/laminin (Sigma-Aldrich, St. Louis, MO, U.S.A.)-coated 96-well plates at a density of 3000 cells per well. After 24 h, the medium was changed to a growth medium containing 0.2% dimethyl sulfoxide (DMSO) and 100 μM of temozolomide, cisplatin, etoposide, nimustine, 5-fluorouracil, methotrexate, tamoxifen, all-*trans* retinoic acid (Wako Pure Chemical Corporation, Osaka, Japan) and irinotecan (LKT Laboratories, St. Paul, MN, U.S.A.). After 3 d, 10 μL of Cell Counting Kit-8 (Dojindo, Kumamoto, Japan) reagent was added to each well, and cells were incubated for 4 h at 37 °C. The absorbance was then measured at 450 nm using a 2030 ARVO X Multilabel Reader (PerkinElmer, Inc., Life and Analytical Sciences, Waltham, MA, U.S.A.).

RT-PCR and Real-Time Quantitative PCR (qPCR) Total RNA was extracted with TRIzol reagent (Ambion, ThermoFisher Scientific) and purified using the PureLink RNA Mini Kit (Ambion, ThermoFisher Scientific). First-strand cDNA was synthesized from 2 μg of total RNA using SuperScript III reverse transcriptase (Invitrogen, Thermo Fisher Scientific) with oligo$(dT)_{12\text{-}18}$ primer (Invitrogen) in a volume of 20 μL and used as template cDNA for subsequent PCR reaction.

RT-PCR was performed with template cDNA (30 ng), ExTaqHS (TaKaRa Bio, Shiga, Japan) in a 25 μL reaction using a Mastercycler Gradient thermal cycler (Eppendorf, Hamburg, Germany) according to the following protocol: ini-

tial denaturation at 94 °C for 30 s, followed by 20–34 cycles of denaturation at 98 °C for 10 s, annealing at 58–60 °C for 30 s and extension at 72 °C for 45 s. The final extension was carried out at 72 °C for 3 min. Specific primers (Fasmac, Kanagawa, Japan), annealing temperature, and the number of cycles for each reaction are listed in Supplementary Table 2. The absence of genomic contamination was confirmed by using reverse transcriptase-negative samples.

Real-time qPCR was carried out using StepOne Real-Time PCR system (Applied Biosystems, Foster City, CA, U.S.A.). The PCR reaction mixture consists of first-strand cDNA (20 ng), 10 μL of FastStart Universal Probe Master (Roche Applied Science, Indianapolis, IN, U.S.A.), 200 nM gene-specific forward and reverse primers (Fasmac), and 200 nM Universal Probe Library Probes (Universal Probe Library Human Set, Roche Applied Science) in 20 μL reaction volume. PCR conditions were initially set at 95 °C for 10 min, followed by 50 cycles of 95 °C for 15 s and 60 °C for 1 min. Specific primers and Universal Probes were listed in Supplementary Table 3. Experiments were performed in triplicate using the delta–delta Ct method, and glyceraldehyde-3-phosphate dehydrogenase was used as an endogenous control to normalize expression data.

DNA Microarray The integrity of total RNA isolated from U87MG ($n=3$) and P4E8 ($n=3$) cells was assessed using a BioAnalyzer 2100 (Agilent Technologies, Waldbronn, Germany), and no degradation was observed. Microarray analysis was performed by Hokkaido System Science (Sapporo, Japan) using the SurePrint G3 Human 8x60K ver. 2.0 (Agilent, Santa Clara, CA, U.S.A.). The data analysis was performed with GeneSpring GX. The raw data were normalized with a 75 percentile shift, and baseline transformation was performed using the median of all samples. Subsequently, the relative expression of each gene was analyzed. The data have been deposited in the NCBI Gene Expression Omnibus (GEO) database (GSE146698).

Immunohistochemistry This study was performed following the ethical principles for medical research outlined in the Declaration of Helsinki and relevant guidelines and regulations. Written informed consent was obtained from each patient and this study was approved by the Institutional Review Board of Kansai Medical University (No. 1401-1, 2017085).

Tumor specimens were obtained from patients with glioma by surgical resection at the department of neurosurgery, Kansai Medical University. Formalin-fixed paraffin-embedded blocks of human glioma tissues were cut into 5 μm-thick sections and mounted on glass slides. Sections were deparaffinized in xylene and rehydrated in a graded series of ethanol. The sections were then immersed in 20 mM sodium citrate buffer (pH 6) and antigen retrieval was performed by autoclave heating at 120 °C for 20 min. After blocking with Blockace, sections were incubated overnight at 4 °C with rabbit polyclonal antibodies against Sox2 (1 : 1000 dilution) or MSMP (1 : 200 dilution) (Supplementary Table 1), followed by treatment with anti-rabbit immunoglobulin G (IgG) biotinylated goat IgG (1 : 100 dilution, Vector Laboratories, Burlingame, CA, U.S.A.). Then, sections were incubated with avidin-biotin-peroxidase complex (ABC) reagent (VECTASTAIN ABC-Kit, Vector Laboratories) and visualized using ImmPACT DAB (Vector Laboratories). Images were captured using a Nikon Eclipse Ni light microscope (Nikon, Tokyo, Japan) under bright-field illumination.

Statistical Analysis The data for tumor growth *in vivo* were analyzed by two-way repeated measures ANOVA with Bonferroni *post hoc* test using GraphPad Prism v.4.03 software (GraphPad Software Inc., San Diego, CA, U.S.A.). The comparison of drug sensitivity between U87MG and P4E8 cells was performed by two-sided Welch's *t*-test using Microsoft Excel version 2013.

RESULTS

Establishment of Single Cell-Derived Tumorsphere from U87MG Cell Line It had been reported that CSC-like cells were isolated from several human glioblastoma cell lines including U87MG cells, which was widely used in brain tumor research.[21–23] To isolate CSC-like population from U87MG cells, the expression of CSC marker CD133 was first examined by a flow cytometer because CD133 expression was controversial in U87MG cells.[24–26] As shown in Supplementary Fig. 1, the CD133 expression in U87MG cells was not observed. Then, we examined the existence of side population (SP) cells by FACS analysis under adherent and sphere culture condition (Supplementary Fig. 2) because sphere culture was widely used to enrich CSCs. However, since verapamil, an inhibitor of Hoechst33342 transport, did not significantly change the SP cell population in adherent and sphere culture of U87MG cells, it is concluded that CD133-positive cells and SP cells

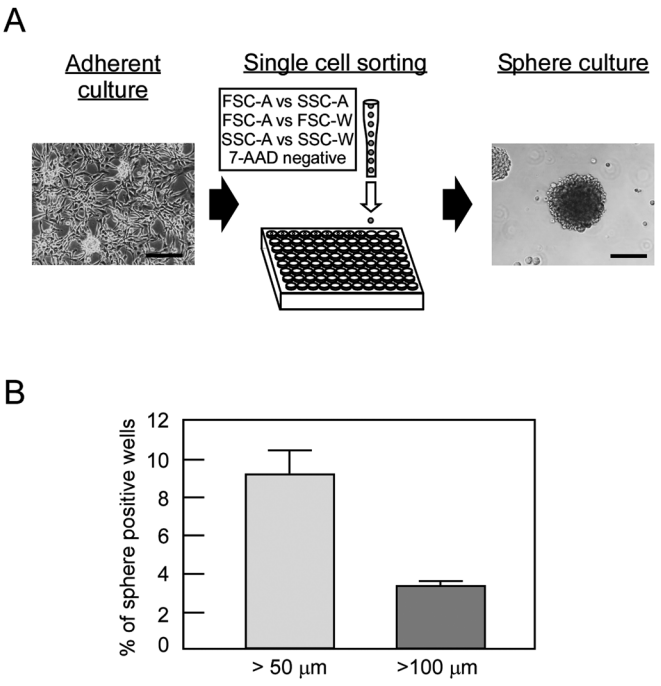

Fig. 1. Establishment of Single Cell-Derived Tumorspheres from U87MG Cells

(A) Schematic representation of establishing single cell-derived tumorspheres. U87MG cells were gated by FSC *vs.* SSC and then singlet cells were selected by two subsequent gates in plot of FSC-A *vs.* FSC-W and SSC-A *vs.* SSC-W. The 7-AAD negative live cells were sorted into each well of 96-well plates (1 cell/well) and further incubated and expanded in neurosphere medium. Representative phase contrast images of adherent U87MG cells and established tumorsphere were shown. Scale bars, 200 μm. (B) Sphere forming efficiency was determined 2-weeks after single-cell sorting. Light and dark gray bars represent the percentage of wells containing spheres more than 50 and 100 μm in diameter, respectively. Data represents the mean ± standard deviation (S.D.) of three separate experiments. A total of 1152 wells were analyzed.

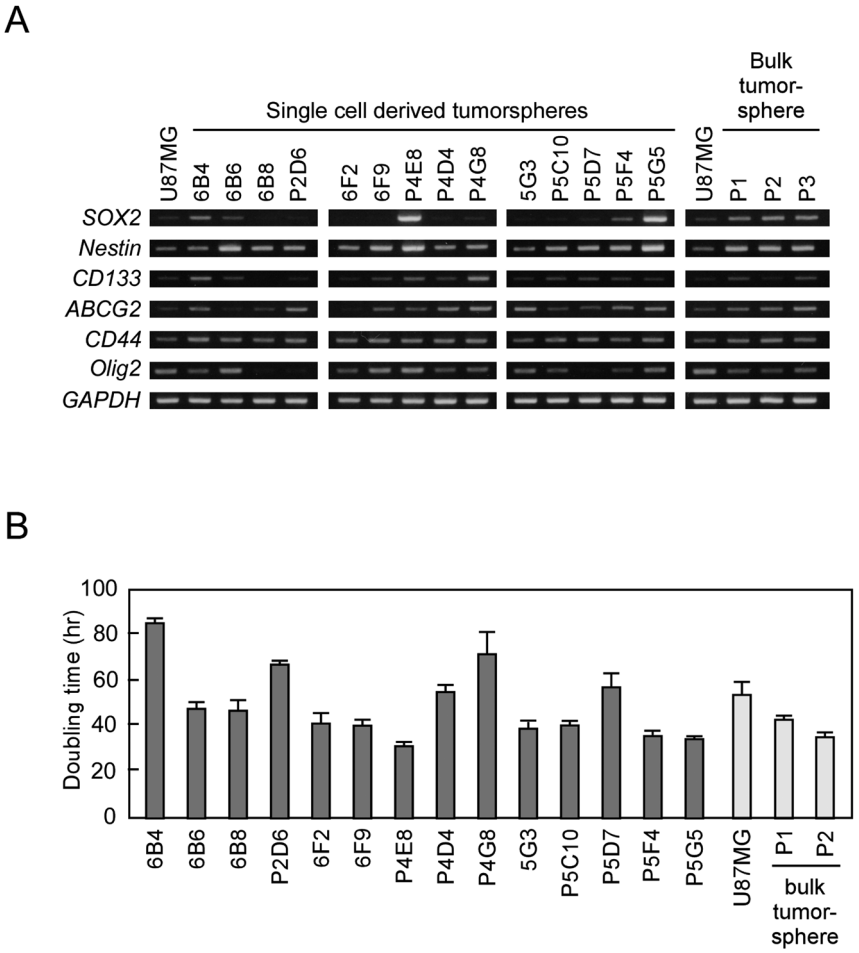

Fig. 2. The mRNA Expression of CSC Markers and Cell Proliferation Rates in Established Tumorspheres

(A) RT-PCR analysis of CSC marker gene expression in established tumorspheres. Bulk tumorsphere means the tumorspheres derived from the bulk U87MG cells. Samples derived from the bulk tumorsphere at passages 1, 2, and 3 are shown as P1, P2, and P3, respectively. The samples from adherent U87MG cells were expressed as U87MG. (B) The population doubling time of each tumorsphere (dark gray), adherent U87MG cells and bulk tumorspheres (light gray) were indicated as the mean ± S.D. of three separate experiments.

were not present in U87MG cells.

Therefore, a single cell-derived sphere formation was employed to isolate the CSC-like population from U87MG cells. Single cells were sorted into 96-well plates (1 cell/well) by FACS and were further incubated in a neurosphere medium for 2 weeks (Fig. 1A). As shown in Fig. 1B, the sphere formation efficiency for >100 and $>50\,\mu$m tumorsphere diameter were 3.3 ± 0.3 and 9.2 ± 1.3%, respectively. Spheres for $>100\,\mu$m tumorsphere diameter were further expanded separately, and 14 of single cell-derived tumorspheres were established.

To characterize the established tumorspheres, gene expression of known CSC markers was analyzed by RT-PCR. As shown in Fig. 2A, the marker expression profile was varied for each tumorsphere. All markers examined were expressed in 6B4, P4E8, P5F4, P5G5, and tumorspheres derived from the bulk U87MG cells (bulk tumorsphere). Among these tumorspheres, especially high expression of both Sox2 and Nestin were seen in P4E8 and P5G5 tumorsphere. These tumorspheres also had a shorter doubling time (31.7 ± 0.9 h for P4E8, 34.8 ± 0.3 h for P5G5) than others (Fig. 2B). The mRNA expression of Sox2 and Nestin in bulk tumorsphere was slightly higher than that in adherent U87MG cells but lower than in P4E8 and P5G5. These results suggest that bulk tumorsphere was composed of sphere forming cells with distinct CSC marker expression profiles, but the floating culture of the single cell could establish clonal tumorsphere.

Tumorigenic Ability of Established Single Cell-Derived Tumorspheres To evaluate the *in vivo* tumorigenicity, P4E8 and P5G5 tumorspheres were subcutaneously injected into the nude mice because these tumorspheres highly expressed Sox2, which had been reported to be important for tumorigenicity and proliferation of glioblastoma initiating cells.[27] For comparison, U87MG cells under adherent culture condition were also investigated. When 1×10^6 cells were injected, P4E8 cells generated significantly larger tumors than U87MG cells on days 25, 30, and 35 (Figs. 3A, B). Even inoculation of 3×10^5 P4E8 cells tends to form larger tumors than 1×10^6 U87MG cells. On the other hand, P5G5 cells did not generate a tumor until day 35. Furthermore, orthotopic injection of U87MG and P4E8 cells into the brains of nude mice was carried out (Fig. 3C). At 14 d after injection, P4E8 cells formed brain tumors in three out of four mice, but adherent U87MG cells did not.

These results indicated that P4E8 cells have highly tumorigenic and proliferative properties compared to adherent U87MG cells.

Characterization of CSC-Like Properties of P4E8 Tumorsphere To further characterize the CSC-like properties

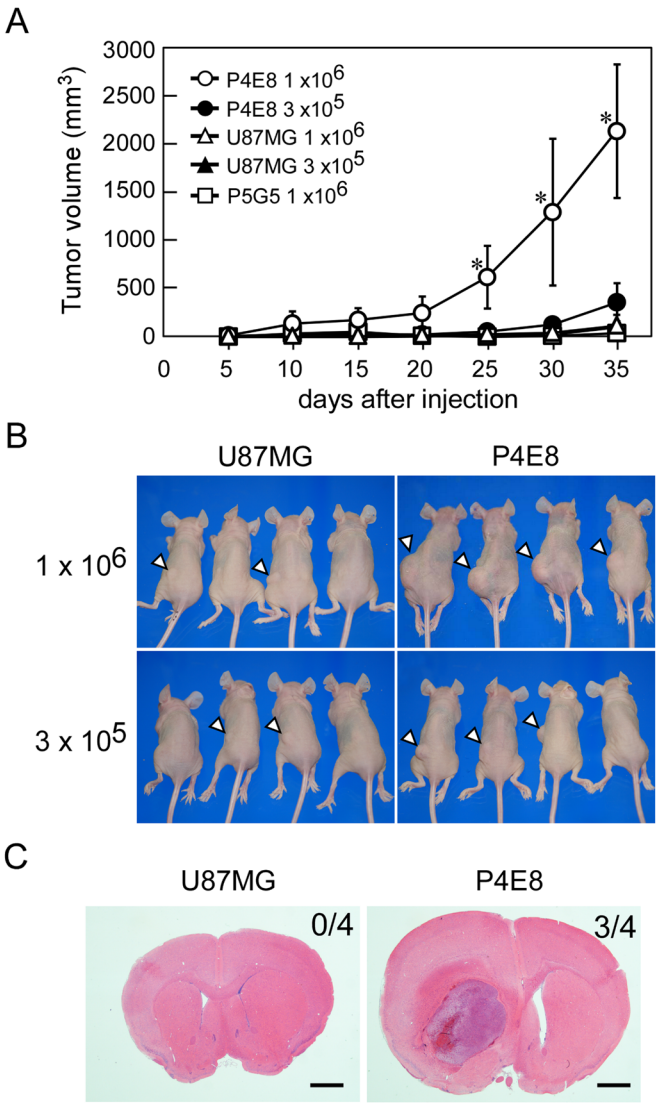

Fig. 3. Tumor Formation Ability of P4E8 Cells after Subcutaneous or Intracranial Injection

Adherent U87MG, P4E8 and P5G5 cells were subcutaneously injected into the left flank of Balb/C nude mice at indicated cell number ($n=4$ mice in each group). (A) After injection, each tumor volume was measured every 5 d. Data represents the mean ± S.D. from four mice per group. Two-way repeated measures ANOVA with Bonferroni *post hoc* test showed significant difference of tumor growth of mice inoculated with P4E8 (1×10^6) cells compared to U87MG cells (1×10^6) (*$p<0.001$). (B) Representative pictures of mice at 35 d after injection with indicated number of U87MG or P4E8 cells were shown. Arrowheads indicate tumors. (C) Representative images of H&E-stained coronal brain sections at 14 d after intracranial injection with U87MG or P4E8 cells ($n=4$ mice per group). Scale bars, 1 mm. Tumor incidence is displayed in the upper right corner of each image. (Color figure can be accessed in the online version.)

of P4E8 cells, the expression of known CSC markers (Sex determining region Y (SRY)-Box2 (Sox2), stage-specific embryonic antigen 1 (SSEA-1), and Nestin) and differentiation markers (S100β, glial fibrillary acidic protein (GFAP), and βIII tubulin) was examined by immunocytochemistry. As shown in Fig. 4A, higher expression of Sox2 and SSEA-1 was observed in P4E8 cells than in U87MG cells. On the other hand, Nestin was expressed in both U87MG and P4E8 cells. For astrocytic markers, S100β was expressed in both U87MG and P4E8 cells, but GFAP was not. For neuronal marker βIII tubulin, weak signals were partially seen in both U87MG and P4E8 cells. Next, the sphere-forming frequency was determined by limiting dilution assay.[20] The number of cells required to generate at least one tumorsphere/well was calculated as 29.7 cells in U87MG cells and 2.6 cells in P4E8 cells, indicating that P4E8 tumorsphere had higher self-renewal ability than U87MG cells (Fig. 4B). Furthermore, P4E8 cells increased resistance against anti-cancer agents, cisplatin, etoposide, 5-fluorouracil, methotrexate, tamoxifen, and all-*trans* retinoic acid, compared with U87MG cells (Fig. 4C), but only temozolomide enhanced cytotoxicity on P4E8 cells. Among these agents, tamoxifen, an anti-estrogen agent, showed the highest cytotoxic activity against P4E8 cells.

Taken together, these results indicated that P4E8 cells have CSC-like properties such as expression of CSC markers, self-renewal ability, and resistance against various anti-cancer agents, in addition to the high tumorigenic ability. Therefore, P4E8 cells were used as a cell-based model of GSCs for further experiments.

Differential Gene Expression Analysis between Parental U87MG Cells and P4E8 Tumorsphere To find new therapeutic targets for CSCs, differentially expressed genes between adherent U87MG and P4E8 tumorsphere were analyzed by cDNA microarray. A total of 3081 genes were differentially expressed at a two-fold cut-off with p-value <0.05, and 1395 upregulated and 1686 downregulated genes were identified (Fig. 5A). The top 10 significantly upregulated genes in P4E8 cells were shown in Table 1. Among these genes, the highest expressed gene was *MSMP*, and the second highest expressed gene was solute carrier family 24 member 3 (*SLC24A3*). A known CSC marker, *Sox2*, was also upregulated in P4E8 cells, supporting the validity of our data. On the other hand, the high expression of the T cell receptor beta constant 1 (*TRBC1*) gene in P4E8 cells would be false positive or artifact because TRBC1 is a T cell receptor component in T lymphocyte. To validate the microarray data, real-time qPCR was performed for *MSMP*, *SLC24A3*, Phospholipase A2 receptor 1 (*PLA2R1*), FYVE, RhoGEF and PH domain containing 4 (*FGD4*), Prickle homolog 1 (Drosophila) (*PRICKLE1*), *Sox2*, Contactin associated protein-like 3 (*CNTNAP3*), and Potassium voltage-gated channel interacting protein 3 (*KCNIP3*) (Fig. 5B). It is difficult to distinguish between *CNTNAP3* and *CNTNAP3B* gene by PCR analysis because these genes are paralogs with high sequence similarity; therefore, *CNTNAP3B* transcripts would also be amplified by the primer set for *CNTNAP3*. As shown in Fig. 5B, all transcripts were highly expressed in P4E8 cells compared with U87MG cells, supporting the microarray results, although *SLC24A3*, *PRICKLE1*, and *KCNIP3* transcripts were undetected in U87MG cells. In addition, when the expression of these transcripts in P4E8 cells was compared with that in human neural stem cells (hNSC), used as a normal stem cells, the expression of *MSMP, SLC24A3, PLA2R1*, and *KCNIP3* transcripts were higher in P4E8 cells than in hNSC.

Expression of MSMP in Patient-Derived GSC Lines and Human Glioma Tissues Recent evidence showed that GBM could be classified into at least four molecular subtypes.[28] Among these subtypes, proneural and mesenchymal subtypes were mutually exclusive and the mesenchymal subtype displayed a more malignant phenotype than proneural subtype. In the previous report, patient-derived GSCs, 146 and MD13, were molecularly characterized and assigned to proneural and mesenchymal subtype, respectively.[19]

First, the CSC marker expression pattern was compared

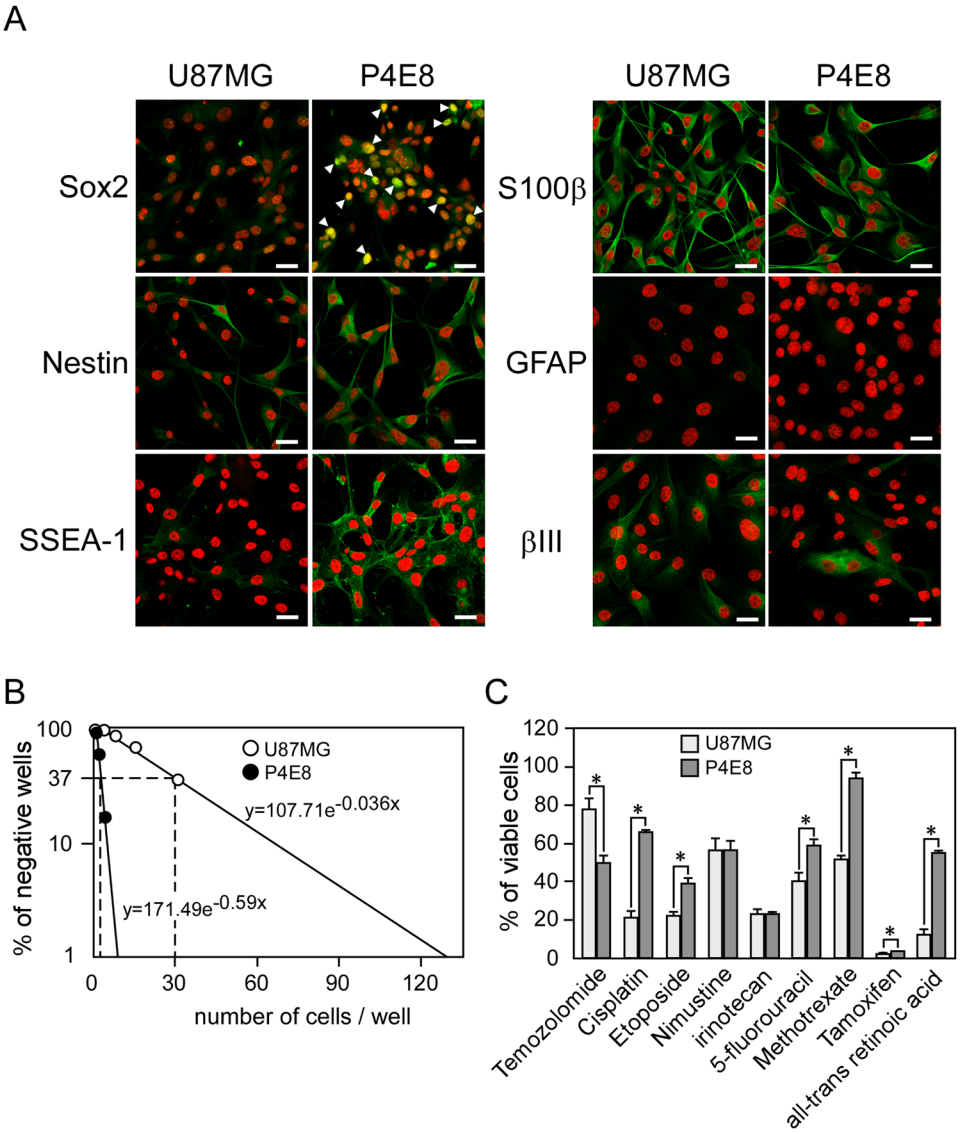

Fig. 4. Characterization of CSC-Like Properties in P4E8 Cells

(A) Immunocytochemical analysis for marker expression in U87MG and P4E8 cells. The fluorescence signals derived from CSC markers (Sox2, Nestin, SSEA-1), astrocyte markers (S100*β* and GFAP) and neuronal marker (*β*III tubulin) were indicated by green. Nuclei were stained with Hoechst33342 (red pseudo-color). Arrowheads indicate Sox2 positive cells. Scale bars, 20 μm. (B) *In vitro* limiting dilution assay of U87MG and P4E8 cells. (C) Drug sensitivity against various chemotherapeutic drugs in U87MG and P4E8 cells. Cells were treated with indicated anti-cancer agents at 100 μM for 3 d. Data represent the mean ± S.D. of three separate experiments. Statistical difference was determined by Welch's *t*-test. Asterisks indicate significant difference between U87MG and P4E8 cells (* $p < 0.01$). (Color figure can be accessed in the online version.)

between P4E8 cells and patient-derived GSCs by immunocytochemistry. SSEA1, highly expressed in P4E8 cells (Fig. 4A), was not expressed in both MD13 and 146 cells (Fig. 6A). On the other hand, Sox2 was more highly expressed in 146 cells than in P4E8 and MD13 cells (Figs. 4A, 6A). These results indicated that the CSC marker expression pattern was different among P4E8, proneural and mesenchymal GSCs.

Next, we determined the expression of *MSMP, SLC24A3, PLA2R1*, and *KCNIP3* in patient-derived GSCs. Among these genes, mRNA expression of *MSMP*, *SLC24A3* and *KCNIP3* were detected in 146 and MD13 cells, but *PLA2R1* transcripts was not (Supplementary Fig. 3A). We further examined the protein expression of SLC24A3 and KCNIP3 by Western blot analysis. As shown in Supplementary Fig. 3B, a significant expression of SLC24A3 was detected in MD13 cells compared with that in P4E8 cells. For KCNIP3, the expression was not detected in the examined cell lines (Supplementary Fig. 3C). The protein expression of MSMP was examined in U87MG, P4E8, and patient-derived GSCs. As shown in Fig. 6B, MSMP showed a punctate pattern in the cytosol of all these cells examined, indicating the localization of MSMP in secretory vesicles (Fig. 6B). Although strong signals were observed in P4E8 and MD13 cells, MSMP was also expressed in U87MG cells. These results suggested that MSMP would be expressed in both GSC and non-GSC but at higher levels in GSC.

Finally, MSMP expression was examined in human glioma tissues graded from I to IV by immunohistochemistry. As shown in Fig. 7, MSMP was detected in the cytoplasm in a punctate pattern in all grade glioma. On the other hand, the expression of Sox2 was higher in high-grade glioma (grades III, IV) compared with low-grade glioma (grades I, II). These results indicated that MSMP was actually expressed in human glioma tissues regardless of glioma grade.

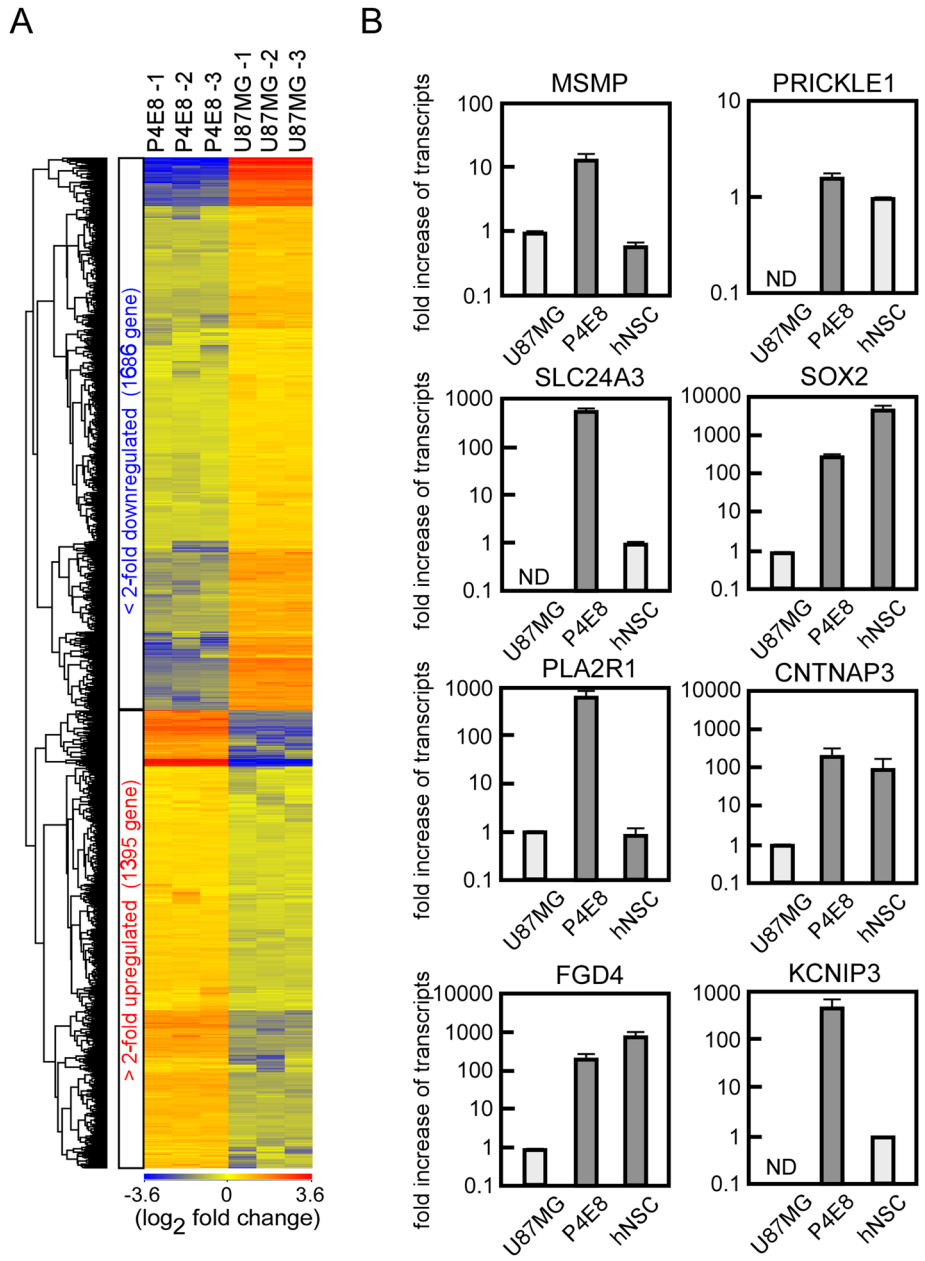

Fig. 5. Differential Gene Expression Analysis between U87MG Cells and P4E8 Tumorsphere by DNA Microarray and Validation of Microarray Data by Real-Time qPCR

(A) The heat map shows 1395 upregulated (>2-fold) and 1686 downregulated (<2-fold) genes in P4E8 tumorspheres compared to U87MG cells in biological triplicates. (B) Validation of DNA microarray experiments by real-time qPCR. In addition to U87MG and P4E8 cells, hNSC was used as a normal stem cells. Each bar indicates fold-increase of transcripts compared with the level of expression in U87MG or hNSC (light gray), which is set at a value of 1. Data represent the mean ± S.D. from three separate experiments. ND, not detected. (Color figure can be accessed in the online version.)

Table 1. Top 10 Genes Up-Regulated in P4E8 Cells (*versus* U87MG Cells)

Accession No.	Descriptions	Fold change	*p*-Value
NM_001044264	Microseminoprotein, prostate associated (*MSMP*)	622.1	<0.0001
NM_020689	Solute carrier family 24 member 3 (*SLC24A3*)	552.8	<0.0001
ENST00000610439	T cell receptor beta constant 1 (*TRBC1*)	375.1	<0.0001
NM_003106	SRY-box 2 (*SOX2*)	344.2	<0.0001
NM_139241	FYVE, RhoGEF and PH domain containing 4 (*FGD4*)	200.1	<0.0001
NM_013434	Potassium voltage-gated channel interacting protein 3 (*KCNIP3*)	178.7	<0.0001
NM_001201380	Contactin associated protein-like 3B (*CNTNAP3B*)	154.1	<0.0001
NM_033655	Contactin associated protein-like 3 (*CNTNAP3*)	122.0	<0.0001
NM_153026	Prickle homolog 1 (Drosophila) (*PRICKLE1*)	118.0	<0.0001
NM_007366	Phospholipase A2 receptor 1, 180 kDa (*PLA2R1*)	112.7	<0.0001

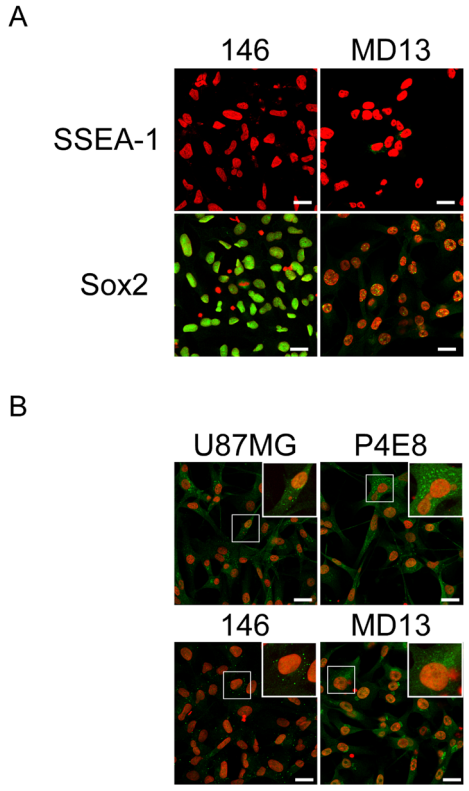

Fig. 6. The Protein Expression of MSMP in Patient-Derived GSCs (146 and MD13 Cells)

(A) Immunocytochemical analysis of SSEA-1 and Sox2 expression in patient-derived GSCs. The fluorescence signals derived from SSEA1 and Sox2 were indicated by green. Nuclei were stained with Hoechst33342 (red pseudo-color). Scale bars, 20 μm. (B) Immunocytochemical analysis of MSMP expression in patient-derived GSCs. The fluorescence signals derived from MSMP were indicated by green. Nuclei were stained with Hoechst33342 (red pseudo-color). The inset in the upper right corner of each image shows magnified image of boxed area. Scale bars, 20 μm. (Color figure can be accessed in the online version.)

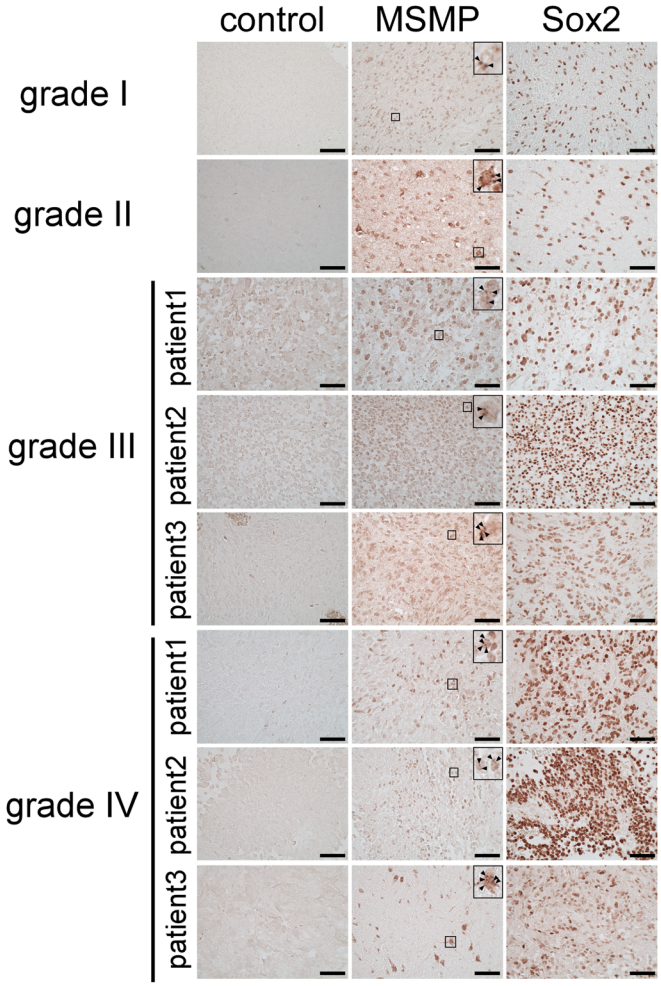

Fig. 7. Immunohistochemical Analysis of MSMP and Sox2 Expression in Glioma Tissues

Tissue sections were immunostained with no antibody (control), anti-MSMP antibody (MSMP) or anti-Sox2 antibody (Sox2). Glioma grades were pathologically determined according to the WHO criteria. Grade I, pilocytic astrocytoma; Grade II, oligoastrocytoma; Grade III, anaplastic pilocytic astrocytoma (patient 1), anaplastic oligoastrocytoma (patient 2), anaplastic astrocytoma (patient 3); Grade IV, glioblastoma (patients 1–3). For MSMP immunohistochemistry, the inset in the upper right corner of each image shows magnified image of boxed area. Arrowheads in the inset indicate the distribution of MSMP as vesicle-like puncta in the cytoplasm. Scale bars, 50 μm. (Color figure can be accessed in the online version.)

DISCUSSION

Targeted therapies against CSCs are considered to be a promising therapeutic strategy. However, identification and isolation of CSCs from tumor tissues have still been challenging because of a rare population and phenotypic heterogeneity of CSCs. Even in the same human GBM tissue, CSCs derived from the periphery or core region had distinct properties such as proliferation potential and tumor-initiating ability.[29,30] Since CSC heterogeneity is also implicated in the difficulties of CSC-targeted therapy,[31] exploring more target molecules of CSCs is important for further clinical implication.

We established tumorspheres from human glioblastoma U87MG cells by the floating culture of single cell in the neurosphere medium. Among established tumorspheres, P4E8 cells were considered a cell-based model of GSCs because P4E8 cells showed CSC-like phenotypes such as self-renewal ability, expression of CSC markers, drug resistance, and high tumorigenic potential.

CSCs were known to be resistant to anti-cancer drugs. One of the cause of drug resistance is an overexpression of ATP-binding cassette (ABC)-transporter family such as P-glycoprotein (P-gp), multidrug resistance-associated proteins (MRPs) and breast cancer resistance protein (BCRP).[32,33] We showed that P4E8 cells were resistance to cisplatin, etoposide, 5-fluorouracil, methotrexate, tamoxifen and all-*trans* retinoic acid (Fig. 4C). Among these agents, cisplatin, etoposide, 5-FU, methotrexate, tamoxifen had been reported to be substrates of ABC transporters.[34] Although temozolomide and SN-38 (the active metabolite of irinotecan) had been reported to be substrates of ABC transporer,[34,35] P4E8 cells did not show the drug resistance against these agents. These results suggested the contribution of particular ABC transporters to drug resistance in P4E8 cells. In addition, P4E8 cells showed resistance against all-*trans* retinoic acid, which is not a substrate of ABC transporter, implying the involvement of other drug resistance mechanism. Thus, it is considered that not only ABC transporters but also other mechanism would contribute to the drug resistance of P4E8 cells. On the other hand, since significant cytotoxic activity against P4E8 cells was observed in treatment with tamoxifen (Fig. 4C), this drug might be a good candidate for GSC-targeted therapy. Thus, the cell-based model of CSC is useful for screening for CSC-targeting agents. In addition, single cell-derived tumorsphere formation would also be useful for isolation of CSC from tumor tissues by not being

dependent on the expression of cell surface markers.

As shown in Fig. 2A, both P4E8 and P5G5 showed higher mRNA expression of Sox2 compared with other established tumorspheres, but only P4E8 cells formed tumors (Fig. 3A). It had been reported that the Sox2 protein function were regulated through various post-translational modifications such as phosphorylation, acetylation, methylation, SUMOlylation, and ubiquitylation.[36] Therefore, the different post-translational modifications of Sox2 between P4E8 and P5G5 cells may contribute to the different tumorigenicity *in vivo*. Sox2 is known to be a CSC marker of proneural subtype but not of mesenchymal subtype.[37] Immunocytochemical analysis revealed that the expression of Sox2 in P4E8 cells was comparable to mesenchymal MD13 cells but was lower than that in proneural 146 cells (Figs. 4A, 6A). These results suggest that P4E8 cells would not be a proneural subtype.

We identified highly expressed genes in P4E8 cells compared to the parental U87MG by microarray analysis. Among these genes, the expression of *MSMP, SLC24A3, PLA2R1*, and *KCNIP3* transcripts were higher in P4E8 cells than in normal hNSC, but the expression of PLA2R1 transcripts and KCNIP3 protein were undetected in patient-derived GSC (Supplementary Fig. 3). On the other hand, a significant expression of SLC24A3 was detected in MD13 cells compared with that in P4E8 cells. Although further studies are required, these results suggest that SLC24A3 may be involved in the function of mesenchymal GSCs.

The human *MSMP* gene, encoding an 11.1 kDa secretory protein, had been identified by sequence similarity to human β-microseminoprotein.[38] Although the expression of MSMP mRNA in normal human tissues was limited to trachea and testis, MSMP transcripts and protein were highly expressed in prostate cancer cell line PC-3.[38] In addition, the immunohistochemical analysis had indicated the high level expression of MSMP in human benign prostatic hyperplasia, prostate cancers and breast tumor tissues.[38,39] This study first indicated that MSMP was expressed in patient-derived GSCs (146 and MD13) and human glioma tissues.

The secretion of endogenous MSMP had previously been determined in human prostate cancer PC-3 cells[38,39] and human ovarian cancer cell lines.[40] To determine the secretion of MSMP from U87MG, P4E8, and PC-3 cells, culture medium was harvested after 48 h incubation of 1×10^6 cells in 6 well plates and the enzyme-linked immunosorbent assay was performed (data not shown). As a result, the secreted MSMP was undetectable level in the culture medium of all these cell lines including PC-3 cells. Since MSMP has been well known to be secreted from PC-3 cells, further detailed investigation of experimental condition is required to determine the secretion of MSMP in U87MG and P4E8 cells. On the other hand, it had been reported that MSMP expression and secretion was low under normoxic condition but high under hypoxic condition in ovarian cancer cell lines,[40] suggesting that the secretion of MSMP from P4E8 cells may also be induced under hypoxic condition.

Although the functions of MSMP are not fully understood, it had been reported that MSMP had a chemoattractant activity toward peripheral blood monocytes through C-C chemokine receptor 2 (CCR2), the receptor of monocyte chemoattractant protein 1 (MCP-1).[39] In solid tumors, tumor-associated macrophages (TAMs), a component of the tumor microenvironment, have been implicated in promoting tumor progression and associated with poor prognosis.[41,42] Therefore, it is speculated that MSMP expressed from glioma cells, including GSCs, may increase the recruitment of monocytes from the circulation, resulting in the increase of the number of TAMs and enhancement of glioma progression.

Although the functional analysis was required to elucidate the role of MSMP in glioma progression, our findings raise the possibility that MSMP may contribute to glioma development or progression, or both.

Acknowledgments The authors thank Fumio Yamashita and Tetsuji Yamamoto (Kansai Medical University, Osaka, Japan) for technical assistance and Yuki Okada (Kansai Medical University, Osaka, Japan) for expert secretarial work. We appreciate Prof. Ichiro Nakano (University of Alabama at Birmingham) for providing patient-derived GSCs. This work was supported by Grant-in-Aid for Scientific Research (C) (Grant Nos. 25460049, 17K07183) from the Japan Society for the Promotion of Science (JSPS) and the research Grants from Kansai Medical University.

Conflict of Interest The authors declare no conflict of interest.

Supplementary Materials The online version of this article contains supplementary materials.

REFERENCES

1) Stupp R, Hegi ME, Mason WP, *et al.* Effects of radiotherapy with concomitant and adjuvant temozolomide *versus* radiotherapy alone on survival in glioblastoma in a randomised phase III study: 5-year analysis of the EORTC-NCIC trial. *Lancet Oncol.*, **10**, 459–466 (2009).
2) Gilbert CA, Ross AH. Cancer stem cells: cell culture, markers and targets for new therapies. *J. Cell. Biochem.*, **108**, 1031–1038 (2009).
3) Reya T, Morrison SJ, Clarke MF, Weissman IL. Stem cells, cancer, and cancer stem cells. *Nature*, **414**, 105–111 (2001).
4) Beier D, Hau P, Proescholdt M, Lohmeier A, Wischhusen J, Oefner PJ, Aigner L, Brawanski A, Bogdahn U, Beier CP. CD133(+) and CD133(−) glioblastoma-derived cancer stem cells show differential growth characteristics and molecular profiles. *Cancer Res.*, **67**, 4010–4015 (2007).
5) Chen R, Nishimura MC, Bumbaca SM, *et al.* A hierarchy of self-renewing tumor-initiating cell types in glioblastoma. *Cancer Cell*, **17**, 362–375 (2010).
6) Ho MM, Ng AV, Lam S, Hung JY. Side population in human lung cancer cell lines and tumors is enriched with stem-like cancer cells. *Cancer Res.*, **67**, 4827–4833 (2007).
7) Kondo T, Setoguchi T, Taga T. Persistence of a small subpopulation of cancer stem-like cells in the C6 glioma cell line. *Proc. Natl. Acad. Sci. U.S.A.*, **101**, 781–786 (2004).
8) Wu CP, Zhou L, Xie M, Du HD, Tian J, Sun S, Li JY. Identification of cancer stem-like side population cells in purified primary cultured human laryngeal squamous cell carcinoma epithelia. *PLOS ONE*, **8**, e65750 (2013).
9) Broadley KW, Hunn MK, Farrand KJ, Price KM, Grasso C, Miller RJ, Hermans IF, McConnell MJ. Side population is not necessary or sufficient for a cancer stem cell phenotype in glioblastoma multiforme. *Stem Cells*, **29**, 452–461 (2011).
10) Dontu G, Abdallah WM, Foley JM, Jackson KW, Clarke MF, Kawamura MJ, Wicha MS. *In vitro* propagation and transcriptional profiling of human mammary stem/progenitor cells. *Genes Dev.*, **17**,

1253–1270 (2003).
11) Booth BW, Boulanger CA, Smith GH. Alveolar progenitor cells develop in mouse mammary glands independent of pregnancy and lactation. *J. Cell. Physiol.*, **212**, 729–736 (2007).
12) Liao MJ, Zhang CC, Zhou B, Zimonjic DB, Mani SA, Kaba M, Gifford A, Reinhardt F, Popescu NC, Guo W, Eaton EN, Lodish HF, Weinberg RA. Enrichment of a population of mammary gland cells that form mammospheres and have *in vivo* repopulating activity. *Cancer Res.*, **67**, 8131–8138 (2007).
13) Chen YC, Ingram PN, Fouladdel S, McDermott SP, Azizi E, Wicha MS, Yoon E. High-throughput single-cell derived sphere formation for cancer stem-like cell identification and analysis. *Sci. Rep.*, **6**, 27301 (2016).
14) Pang L, Ding J, Ge Y, Fan J, Fan SK. Single-cell-derived tumorsphere formation and drug-resistance assay using an integrated microfluidics. *Anal. Chem.*, **91**, 8318–8325 (2019).
15) Takaya A, Hirohashi Y, Murai A, Morita R, Saijo H, Yamamoto E, Kubo T, Nakatsugawa M, Kanaseki T, Tsukahara T, Tamura Y, Takemasa I, Kondo T, Sato N, Torigoe T. Establishment and analysis of cancer stem-like and non-cancer stem-like clone cells from the human colon cancer cell line SW480. *PLOS ONE*, **11**, e0158903 (2016).
16) Vermeulen L, Todaro M, de Sousa Mello F, Sprick MR, Kemper K, Perez Alea M, Richel DJ, Stassi G, Medema JP. Single-cell cloning of colon cancer stem cells reveals a multi-lineage differentiation capacity. *Proc. Natl. Acad. Sci. U.S.A.*, **105**, 13427–13432 (2008).
17) Liu H, Zhang W, Jia Y, Yu Q, Grau GE, Peng L, Ran Y, Yang Z, Deng H, Lou J. Single-cell clones of liver cancer stem cells have the potential of differentiating into different types of tumor cells. *Cell Death Dis.*, **4**, e857 (2013).
18) Meyer M, Reimand J, Lan X, Head R, Zhu X, Kushida M, Bayani J, Pressey JC, Lionel AC, Clarke ID, Cusimano M, Squire JA, Scherer SW, Bernstein M, Woodin MA, Bader GD, Dirks PB. Single cell-derived clonal analysis of human glioblastoma links functional and genomic heterogeneity. *Proc. Natl. Acad. Sci. U.S.A.*, **112**, 851–856 (2015).
19) Mao P, Joshi K, Li J, Kim SH, Li P, Santana-Santos L, Luthra S, Chandran UR, Benos PV, Smith L, Wang M, Hu B, Cheng SY, Sobol RW, Nakano I. Mesenchymal glioma stem cells are maintained by activated glycolytic metabolism involving aldehyde dehydrogenase 1A3. *Proc. Natl. Acad. Sci. U.S.A.*, **110**, 8644–8649 (2013).
20) Tropepe V, Sibilia M, Ciruna BG, Rossant J, Wagner EF, van der Kooy D. Distinct neural stem cells proliferate in response to EGF and FGF in the developing mouse telencephalon. *Dev. Biol.*, **208**, 166–188 (1999).
21) Qiang L, Yang Y, Ma YJ, Chen FH, Zhang LB, Liu W, Qi Q, Lu N, Tao L, Wang XT, You QD, Guo QL. Isolation and characterization of cancer stem like cells in human glioblastoma cell lines. *Cancer Lett.*, **279**, 13–21 (2009).
22) Yu SC, Ping YF, Yi L, Zhou ZH, Chen JH, Yao XH, Gao L, Wang JM, Bian XW. Isolation and characterization of cancer stem cells from a human glioblastoma cell line U87. *Cancer Lett.*, **265**, 124–134 (2008).
23) Iacopino F, Angelucci C, Piacentini R, Biamonte F, Mangiola A, Maira G, Grassi C, Sica G. Isolation of cancer stem cells from three human glioblastoma cell lines: characterization of two selected clones. *PLOS ONE*, **9**, e105166 (2014).
24) Platet N, Liu SY, Atifi ME, Oliver L, Vallette FM, Berger F, Wion D. Influence of oxygen tension on CD133 phenotype in human glioma cell cultures. *Cancer Lett.*, **258**, 286–290 (2007).
25) Christensen K, Aaberg-Jessen C, Andersen C, Goplen D, Bjerkvig R, Kristensen BW. Immunohistochemical expression of stem cell, endothelial cell, and chemosensitivity markers in primary glioma spheroids cultured in serum-containing and serum-free medium. *Neurosurgery*, **66**, 933–947 (2010).
26) Wang D, Guo Y, Li Y, Li W, Zheng X, Xia H, Mao Q. Detection of CD133 expression in U87 glioblastoma cells using a novel anti-CD133 monoclonal antibody. *Oncol. Lett.*, **9**, 2603–2608 (2015).
27) Gangemi RM, Griffero F, Marubbi D, Perera M, Capra MC, Malatesta P, Ravetti GL, Zona GL, Daga A, Corte G. Sox2 silencing in glioblastoma tumor-initiating cells causes stop of proliferation and loss of tumorigenicity. *Stem Cells*, **27**, 40–48 (2009).
28) Verhaak RG, Hoadley KA, Purdom E, *et al.* Integrated genomic analysis identifies clinically relevant subtypes of glioblastoma characterized by abnormalities in PDGFRA, IDH1, EGFR, and NF1. *Cancer Cell*, **17**, 98–110 (2010).
29) Piccirillo SG, Combi R, Cajola L, Patrizi A, Redaelli S, Bentivegna A, Baronchelli S, Maira G, Pollo B, Mangiola A, DiMeco F, Dalprà L, Vescovi AL. Distinct pools of cancer stem-like cells coexist within human glioblastomas and display different tumorigenicity and independent genomic evolution. *Oncogene*, **28**, 1807–1811 (2009).
30) Piccirillo SG, Dietz S, Madhu B, Griffiths J, Price SJ, Collins VP, Watts C. Fluorescence-guided surgical sampling of glioblastoma identifies phenotypically distinct tumour-initiating cell populations in the tumour mass and margin. *Br. J. Cancer*, **107**, 462–468 (2012).
31) Wang A, Chen L, Li C, Zhu Y. Heterogeneity in cancer stem cells. *Cancer Lett.*, **357**, 63–68 (2015).
32) Barbato L, Bocchetti M, Di Biase A, Regad T. Cancer stem cells and targeting strategies. *Cells*, **8**, 926 (2019).
33) Dean M, Fojo T, Bates S. Tumour stem cells and drug resistance. *Nat. Rev. Cancer*, **5**, 275–284 (2005).
34) Pan ST, Li ZL, He ZX, Qiu JX, Zhou SF. Molecular mechanisms for tumour resistance to chemotherapy. *Clin. Exp. Pharmacol. Physiol.*, **43**, 723–737 (2016).
35) Deeley RG, Cole SP. Substrate recognition and transport by multidrug resistance protein 1 (ABCC1). *FEBS Lett.*, **580**, 1103–1111 (2006).
36) Williams CAC, Soufi A, Pollard SM. Post-translational modification of SOX family proteins: Key biochemical targets in cancer? *Semin. Cancer Biol.*, **67**, 30–38 (2020).
37) Bhat KPL, Balasubramaniyan V, Vaillant B, *et al.* Mesenchymal differentiation mediated by NF-κB promotes radiation resistance in glioblastoma. *Cancer Cell*, **24**, 331–346 (2013).
38) Valtonen-André C, Bjartell A, Hellsten R, Lilja H, Härkönen P, Lundwall A. A highly conserved protein secreted by the prostate cancer cell line PC-3 is expressed in benign and malignant prostate tissue. *Biol. Chem.*, **388**, 289–295 (2007).
39) Pei X, Sun Q, Zhang Y, Wang P, Peng X, Guo C, Xu E, Zheng Y, Mo X, Ma J, Chen D, Zhang Y, Zhang Y, Song Q, Guo S, Shi T, Zhang Z, Ma D, Wang Y. PC3-secreted microprotein is a novel chemoattractant protein and functions as a high-affinity ligand for CC chemokine receptor 2. *J. Immunol.*, **192**, 1878–1886 (2014).
40) Mitamura T, Pradeep S, McGuire M, Wu SY, Ma S, Hatakeyama H, Lyons YA, Hisamatsu T, Noh K, Villar-Prados A, Chen X, Ivan C, Rodriguez-Aguayo C, Hu W, Lopez-Berestein G, Coleman RL, Sood AK. Induction of anti-VEGF therapy resistance by upregulated expression of microseminoprotein (MSMP). *Oncogene*, **37**, 722–731 (2018).
41) Komohara Y, Jinushi M, Takeya M. Clinical significance of macrophage heterogeneity in human malignant tumors. *Cancer Sci.*, **105**, 1–8 (2014).
42) Hambardzumyan D, Gutmann DH, Kettenmann H. The role of microglia and macrophages in glioma maintenance and progression. *Nat. Neurosci.*, **19**, 20–27 (2016).